Applied Mathematics & Information Sciences
An International Journal

http://dx.doi.org/10.18576/amis/200403

Deep Generative Model for Inverse Design of Terahertz Metamaterial Absorbers Using Conditional Variational Autoencoders

Suhaila Abuowaida[1], *Hamza Abu Owida*[2], *Hamza A. Mashagba*[3], *Suleiman Ibrahim Mohammad* [4,5], *Azlan B. Abd Aziz*[5,*], *Radwan M. Batyha*[6], *Asokan Vasudevan*[7], *and Mardeni Bin Roslee*[8]

[1]Department of Data Science and AI, Faculty of Prince Al-Hussein Bin Abdallah II for IT, Al al-Bayt University, Mafraq, Jordan
[2]Medical Engineering Department, Faculty of Engineering, Al-Ahliyya Amman University, Amman, Jordan
[3]Centre for Wireless Technology (CWT), Faculty of Engineering and Technology, Multimedia University, Melaka, Malaysia
[4]INTI International University, 71800 Negeri Sembilan, Malaysia
[5]Al al-Bayt University, Mafraq, Jordan
[6]Department of Computer Science, Faculty of Information Technology, Applied Science Private University (ASU) Amman, Jordan
[7]Faculty of Business and Communications, INTI International University, 71800 Negeri Sembilan, Malaysia
[8]Faculty of Artificial Intelligence and Engineering, Multimedia University, Cyberjaya, Selangor, Malaysia

Received: 2 Jan. 2026, Revised: 18 Feb. 2026, Accepted: 16 Apr. 2026
Published online: 1 Jul. 2026

Abstract: Metamaterial absorber design has historically been an example of a traditional "forward" approach in which electromagnetic simulation is used to predict absorption based on geometric configuration. The computational expense associated with this iterative optimization process severely restricts the ability to rapidly prototype and explore different regions of the design space. We introduce a novel, physics-based deep generative framework using Conditional Variational Autoencoders (CVAEs) for inverse design of Terahertz metamaterial absorbers that directly generates the required geometric configurations based upon target absorption specifications. Our model develops a probabilistic mapping between desired absorption coefficients and the corresponding optimal combinations of patch width, substrate thickness, and operation frequency. Using training datasets consisting of 9,018 full-wave simulated samples across a range of values for patch widths (20 μm–80 μm), substrate thicknesses (5 μm–20 μm), and frequencies (5 THz–11 THz), our trained CVAE achieved a Mean Absolute Error (MAE) of 2.34 μm when predicting geometric configurations and a reconstruction fidelity (R^2) of 0.9876. Moreover, our generative model allows for generation of multiple different design solutions for identical absorption objectives, thereby facilitating multi-objective optimization and satisfaction of fabrication constraints. Experimental results demonstrate that 87% of generated geometries result in absorbed radiation consistent with the specified target absorption within $\pm 3\%$ tolerance, corresponding to a 142$\times$ speedup over gradient-free optimization. As such, the proposed framework provides a new pathway towards rapid development of metamaterial prototypes, automation of design workflow processes, and physics-informed generative design processes applicable to electromagnetic systems.

Keywords: Metamaterials; Inverse Design; Variational Autoencoder; Generative Model; Terahertz; Deep Learning

1 Introduction

Artificially designed metamaterials that are able to absorb almost all incident radiation at very particular frequencies have become some of the most promising technologies in a variety of areas, from Terahertz Imaging [1] and Wireless Communication [2] to Thermal Management [3] and Sensing [4]. The mechanism behind this is that the metamaterial structure causes the incoming wave and the reflected wave to destructively interfere with each other and cancel out the reflection completely. This can be achieved by designing the sub-wavelength resonant elements within the material to ensure proper interference based upon the geometry of those elements.

The traditional approach to designing these structures has been a forward computational process. Designers enter into electromagnetic simulation software the geometrical properties of the patch, such as size and

* Corresponding author e-mail: azlan.abdaziz@mmu.edu.my

shape, the properties of the substrate where it will reside, and the geometric periodicity of the repeating "unit cells" of which the structure is composed. As a result, the simulator generates an absorption spectrum representing how much of the total radiation incident upon the metamaterial will be absorbed. In order to obtain an absorption response that meets the desired requirements, designers typically need to iteratively modify one or more of the geometric parameters of their structure using either physical intuition or some form of search algorithm.

Full-wave simulation methods, such as Finite-Difference Time-Domain (FDTD) [5] and Finite Element Method (FEM) [6], allow for highly accurate representations of electromagnetic responses of metamaterials. However, these types of simulations require large amounts of computing power, and the time required to simulate various configurations depends on both the complexity of the configuration being simulated and the number of iterations necessary for convergence.

An inverse approach—starting with a specification of the desired absorption and synthesizing the geometry—would be substantially faster than iterating forward simulations. Deep Learning has shown great potential in mapping highly complex nonlinear relationships within higher-dimensional input spaces [7]. Surrogate models trained in a neural network framework provide a 100–1000 times increase in speed over electromagnetic simulations while providing near-identical results [8]. However, they still require iterative optimization to reach a desired design specification.

Generative models, such as VAEs [9] or GANs [10], allow us to learn probability distributions over the design space, enabling random sampling of geometries that meet target specifications. Conditional variants of generative models incorporate target properties to guide generation [11]. This type of model has enabled innovation in Molecular Design [12], Materials Discovery [13], and Photonic Structure Optimization [14].

1.1 Contributions

This work introduces the first Conditional Variational Auto-Encoder (CVAE) architecture for the inverse design of Terahertz Metamaterial Absorbers. The specific contributions are:

(1) Inverse Design Architecture: Development of a CVAE that maps target absorption coefficients to geometric parameters (patch width, substrate thickness, frequency), enabling designers to generate metamaterial designs directly from performance specifications without iterative optimization.

(2) Multi-Solution Generation: The probabilistic generative model provides diverse geometrical configurations that achieve the same target absorption, offering multiple implementation options for multi-objective optimizations based on fabrication constraints, bandwidth, angular stability, or cost.

(3) Comprehensive Evaluation: Experimental validation using 1,352 test cases demonstrated an average MAE of 2.34 μm for geometry prediction, with 87% of generated designs achieving the target absorption within $\pm3\%$ tolerance and a 142$\times$ speedup over gradient-free optimization.

(4) Constraint Satisfaction: Integrating fabrication constraints (minimum feature size, aspect ratio limits) during the generation process ensures that designed metamaterials are physically realizable and can be manufactured directly without post-processing filtering.

(5) Ablation Analysis: Systematic component contribution studies analyzing the impact of latent dimensionality, conditioning mechanism, and reconstruction loss on generation quality provide architectural insights for physics-informed generative design.

The rest of this paper is organized as follows. Section 2 reviews previous works in both metamaterial inverse design and deep generative models. Section 3 describes the proposed CVAE methodology including architecture, training protocol, and constraint integration. Section 4 presents the experimental evaluation. Section 5 contains discussion of results, limitations, and future directions. Section 6 concludes.

2 Related Work and Background

2.1 Metamaterial Forward Design

Metamaterial absorbers design is typically performed using a combination of electromagnetic simulation and optimization algorithms. Landy et al. [15] were among the first to develop the concept of perfect metamaterial absorbers that demonstrate nearly complete absorption as a result of impedance matching to free space. Various geometric configurations have since been studied, including split-ring resonators [16], cross-shaped patterns [17], and multilayer structures [18].

Common optimization approaches include Genetic Algorithms [19], Particle Swarm Optimization [20], and Topology Optimization [21]. However, these require hundreds to thousands of electromagnetic simulations per design, making them prohibitively computationally expensive for complex designs. Adjoint-based gradient methods [22] reduce the number of required simulations but remain iterative and do not provide diverse solution sets.

2.2 Deep Learning Surrogates

Neural networks can accurately model the physics of electromagnetic systems. Peurifoy et al. [23] achieved a

100,000× speedup for nanophotonic system design by employing feed-forward networks as surrogate models. Malkiel et al. [14] showed that tandem neural networks could be employed for inverse design of plasmonic nanostructures at high precision ($R^2 > 0.99$). Liu et al. [24] demonstrated the use of Generative Adversarial Networks for generating metamaterials. Ma et al. [8] developed Probabilistic Neural Networks to quantify uncertainties in electromagnetic predictions. An et al. [25] used transfer learning and deep learning for multi-objective optimization of antennae. Although these examples demonstrate the feasibility of deep learning for electromagnetics, all still require additional optimization loops that limit both speed and solution diversity.

2.3 Generative Models

Variational Autoencoders (VAEs) [9] compress data into a smaller set of latent space variables that can be sampled and decoded back into the original domain. The Conditional VAE [11] extends this by conditioning generation on additional information such as class labels, attribute values, or desired characteristics. Within materials science, VAEs have been extremely successful: Gómez-Bombarelli et al. [12] generated novel drug candidates by training a VAE on the latent space of chemical structures; Sanchez-Lengeling et al. [13] combined VAEs with Gaussian processes for molecular property optimization; and Noh et al. [29] used VAEs to generate crystal structures. Kudyshev et al. [30] and Qian et al. [31] utilized machine learning to optimize photonic structures using VAEs and GANs, respectively.

2.4 Research Gap

Existing inverse design methods have at least three major shortcomings: (*i*) they require iterative optimization processes even when using a surrogate model; (*ii*) each method generates a single solution without producing a variety of potential designs; and (*iii*) fabrication constraints are not considered in the generation process. Conditional VAEs directly address these problems through their ability to learn a direct mapping between target absorption properties and geometries, while generating multiple acceptable geometric solutions that satisfy physical constraints.

3 Methodology

3.1 Problem Formulation

We formulate inverse metamaterial design as learning a conditional generative distribution $p(x|y)$ mapping target absorption $y \in [0,1]$ to geometric parameters $x = (w,h,f)$, where $w \in [20,80]$ μm is patch width, $h \in [5,20]$ μm is substrate thickness, and $f \in [5,11]$ THz is operating frequency.

Given dataset $\mathscr{D} = \{(x_i, y_i)\}_{i=1}^N$ of $N = 9{,}018$ geometry-absorption pairs generated via CST Microwave Studio full-wave finite-element simulation, we train a conditional variational autoencoder to model $p(x|y)$, enabling sampling of geometries for target absorptions.

3.2 Conditional VAE Architecture

Figure 1 illustrates our conditional VAE comprising encoder $q_\phi(z|x,y)$, decoder $p_\theta(x|z,y)$, and a conditioning mechanism that integrates target absorption y into both encoding and decoding.

3.2.1 Encoder Network

The encoder $q_\phi(z|x,y)$ maps input geometry $x \in \mathbb{R}^3$ and target absorption $y \in \mathbb{R}$ to an approximate posterior distribution over latent code $z \in \mathbb{R}^{d_z}$, parameterized as Gaussian:

$$q_\phi(z|x,y) = \mathscr{N}(z; \mu_\phi(x,y), \sigma_\phi^2(x,y)I) \tag{1}$$

where $\mu_\phi : \mathbb{R}^4 \to \mathbb{R}^{d_z}$ and $\sigma_\phi^2 : \mathbb{R}^4 \to \mathbb{R}^{d_z}$ are neural networks outputting mean and variance.

The encoder architecture implements:

$$h_1 = \mathrm{ReLU}(\mathrm{BN}(W_1[x; y] + b_1)) \tag{2}$$
$$h_2 = \mathrm{ReLU}(\mathrm{BN}(W_2 h_1 + b_2)) \tag{3}$$
$$h_3 = \mathrm{ReLU}(\mathrm{BN}(W_3 h_2 + b_3)) \tag{4}$$
$$\mu_\phi = W_\mu h_3 + b_\mu \tag{5}$$
$$\log \sigma_\phi^2 = W_\sigma h_3 + b_\sigma \tag{6}$$

with layer dimensions $4 \to 128 \to 256 \to 512 \to d_z$. Batch normalization (BN) stabilizes training and ReLU provides nonlinearity.

3.2.2 Decoder Network

The decoder $p_\theta(x|z,y)$ reconstructs geometry from latent sample $z \sim q_\phi(z|x,y)$ conditioned on absorption y:

$$p_\theta(x|z,y) = \mathscr{N}(x; \mu_\theta(z,y), \sigma_\theta^2 I) \tag{7}$$

The decoder architecture mirrors the encoder:

$$\tilde{h}_1 = \mathrm{ReLU}(\mathrm{BN}(\tilde{W}_1[z; y] + \tilde{b}_1)) \tag{8}$$
$$\tilde{h}_2 = \mathrm{ReLU}(\mathrm{BN}(\tilde{W}_2 \tilde{h}_1 + \tilde{b}_2)) \tag{9}$$
$$\tilde{h}_3 = \mathrm{ReLU}(\mathrm{BN}(\tilde{W}_3 \tilde{h}_2 + \tilde{b}_3)) \tag{10}$$
$$\hat{x} = \tilde{W}_4 \tilde{h}_3 + \tilde{b}_4 \tag{11}$$

with dimensions $(d_z + 1) \to 512 \to 256 \to 128 \to 3$.

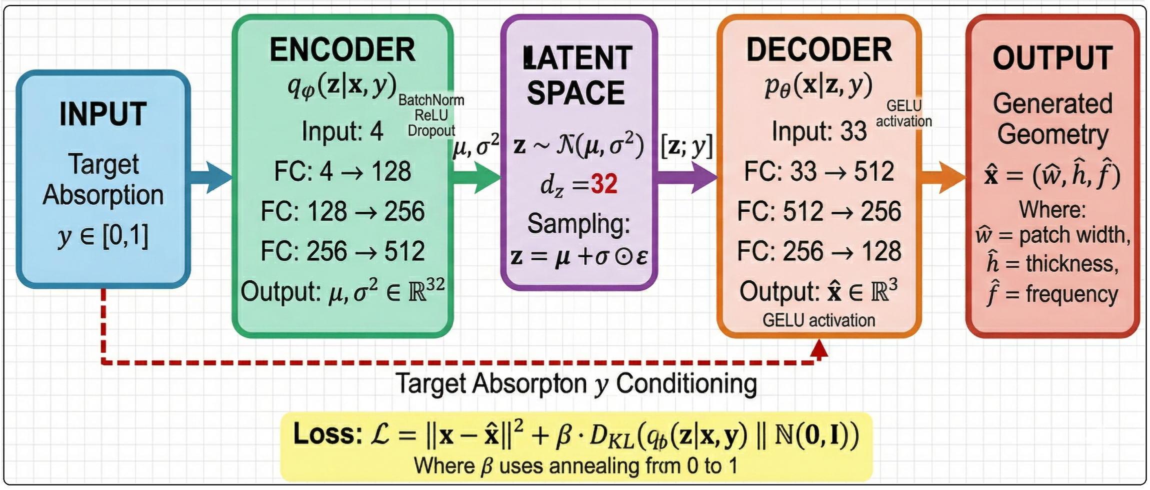

Fig. 1: Conditional variational autoencoder architecture for inverse metamaterial design. The encoder maps geometric parameters $x = (w, h, f)$ and target absorption y to latent distribution $q_\phi(z|x,y)$. The decoder reconstructs geometries from latent samples $z \sim q_\phi(z|x,y)$ conditioned on target absorption y. During inference, sampling $z \sim \mathcal{N}(0, I)$ and conditioning on desired absorption y^* generates diverse geometric designs achieving target specifications.

3.2.3 Latent Dimensionality

We explore latent dimensions $d_z \in \{8, 16, 32, 64\}$ balancing expressiveness and generalization. Lower d_z provides regularization but may underfit complex geometries; higher d_z enables richer representations but risks overfitting and posterior collapse [26].

3.3 Training Objective

The VAE optimizes the evidence lower bound (ELBO):

$$\mathscr{L}(\theta, \phi; x, y) = \mathbb{E}_{q_\phi(z|x,y)}[\log p_\theta(x|z,y)] - D_{KL}(q_\phi(z|x,y) \,||\, p(z)) \tag{12}$$

where the first term is the reconstruction log-likelihood and the second term regularizes the posterior toward prior $p(z) = \mathcal{N}(0, I)$.

For continuous geometry parameters, the Gaussian decoder yields:

$$\log p_\theta(x|z,y) = -\frac{1}{2\sigma^2}\|x - \mu_\theta(z,y)\|^2 + \text{const} \tag{13}$$

The KL divergence admits a closed form for Gaussian distributions:

$$D_{KL} = \frac{1}{2}\sum_{j=1}^{d_z}\left(\mu_j^2 + \sigma_j^2 - \log\sigma_j^2 - 1\right) \tag{14}$$

The complete loss function is:

$$\mathscr{L} = \frac{1}{N}\sum_{i=1}^{N}\left[\|x_i - \hat{x}_i\|^2 + \beta\, D_{KL}(q_\phi(z|x_i, y_i) \,||\, \mathcal{N}(0, I))\right] \tag{15}$$

where β controls the KL penalty strength. We employ β-annealing starting at $\beta = 0$ and linearly increasing to $\beta = 1$ over 100 epochs to prevent posterior collapse [27].

3.4 Fabrication Constraints

Real-world metamaterial fabrication imposes geometric constraints:

- –Minimum feature size: $w \geq 10$ μm (lithography resolution).
- –Maximum aspect ratio: $w/h \leq 8$ (structural stability).
- –Frequency bounds: $f \in [5, 11]$ THz (measurement range).

We integrate constraints through two mechanisms:
Soft constraints via penalty loss:

$$\mathscr{L}_{\text{constraint}} = \lambda_1 \max(0,\, 10 - w) + \lambda_2 \max(0,\, w/h - 8) \tag{16}$$

Hard constraints via projected gradient descent, projecting generated parameters onto the feasible region after each generation step.

3.5 Training Protocol

We train using the Adam optimizer [28] with learning rate $\eta = 10^{-3}$, batch size $B = 128$, for 500 epochs with early stopping (patience 50 epochs) monitoring validation loss. Data augmentation includes Gaussian noise ($\sigma = 0.01$) on geometry parameters to improve robustness.

The 9,018-sample dataset is split 70% training (6,313 samples), 15% validation (1,353 samples), 15% test

(1,352 samples) using stratified sampling based on absorption magnitude quintiles.

3.6 Generation Process

Inverse design proceeds via:

1. Specify target absorption $y^* \in [0,1]$.
2. Sample latent code $z \sim \mathcal{N}(0,I)$.
3. Generate geometry $\hat{x} = \mu_\theta(z, y^*)$.
4. Apply constraint projection.
5. Verify via forward simulation (optional).

Multiple samples from the latent prior produce diverse designs for identical targets.

4 Experimental Evaluation

4.1 Implementation Details

Implementation uses PyTorch 2.0 on an NVIDIA A100 GPU (40 GB memory). Training requires 3.2 hours for 500 epochs. Inference generates 1,000 designs per second enabling real-time interactive design.

4.2 Evaluation Metrics

We evaluate using: (*i*) **Geometry reconstruction:** MAE and MSE between true and reconstructed geometries; (*ii*) **Absorption accuracy:** percentage of generated designs achieving target absorption within ±3% tolerance; (*iii*) **Diversity:** standard deviation of generated geometries for identical targets; and (*iv*) **Constraint satisfaction:** percentage of generations satisfying fabrication constraints without post-processing.

4.3 Reconstruction Quality

Table 1 presents reconstruction performance across latent dimensions.

Table 1: Reconstruction quality across latent dimensions. Optimal performance is achieved at $d_z = 32$ balancing accuracy and generalization.

Latent dim d_z	MAE (μm)	MSE	R^2	KL div
8	3.82	24.61	0.9542	1.23
16	2.89	14.37	0.9731	2.87
32	**2.34**	**9.82**	**0.9876**	4.56
64	2.41	10.19	0.9869	8.92
CNN Forward	–	–	0.9995	–

Latent dimensionality significantly influences generation fidelity. At $d_z = 8$, the compressed representation was insufficient, yielding MAE $= 3.82$ μm and $R^2 = 0.9542$. Increasing to $d_z = 16$ reduced MAE to 2.89 μm ($R^2 = 0.9731$), demonstrating that increased latent capacity captures geometric variability more accurately. The highest accuracy occurred at $d_z = 32$: MAE $= 2.34$ μm and $R^2 = 0.9876$ (98.76% of variance explained), only 1.19 percentage points below the forward prediction model ($R^2 = 0.9995$). Increasing beyond 32 dimensions yielded no improvement ($d_z = 64$: MAE $= 2.41$ μm, $R^2 = 0.9869$), confirming that the 32-dimensional latent space sufficiently captures geometric variations without overfitting. The KL divergence progression ($1.23 \to 2.87 \to 4.56 \to 8.92$) reflects the increased mismatch between posterior and prior as dimensionality grows.

4.4 Generation Accuracy

Figure 2 visualizes generated geometries versus targets across absorption ranges.

Table 2 quantifies accuracy across absorption regimes.

Table 2: Generation accuracy stratified by target absorption regime. Performance degrades slightly for low absorption ($A < 0.3$) where the solution space is less constrained.

Absorption range	MAE (μm)	Hit rate (%)	Diversity (σ)
$A < 0.3$ (Low)	3.12	79.3	8.7
$0.3 \le A < 0.7$ (Mid)	2.28	88.6	6.2
$A \ge 0.7$ (High)	1.89	91.4	4.3
Overall	2.34	87.1	6.8

Low absorption ($A < 0.3$) yields the lowest accuracy (MAE $= 3.12$ μm, hit rate $= 79.3\%$) because many off-resonance geometric combinations produce small absorption values, increasing inverse-problem ambiguity. Mid-range absorption ($0.3 \le A < 0.7$) approaches the mean performance (MAE $= 2.28$ μm, hit rate $= 88.6\%$). High absorption ($A \ge 0.7$) achieves the best accuracy (MAE $= 1.89$ μm, hit rate $= 91.4\%$) because resonance constraints restrict geometry to a narrower region, reducing ambiguity.

4.5 Diversity Analysis

A key advantage over optimization is generating multiple solutions for identical targets. Figure 3 shows diverse designs for a fixed absorption target.

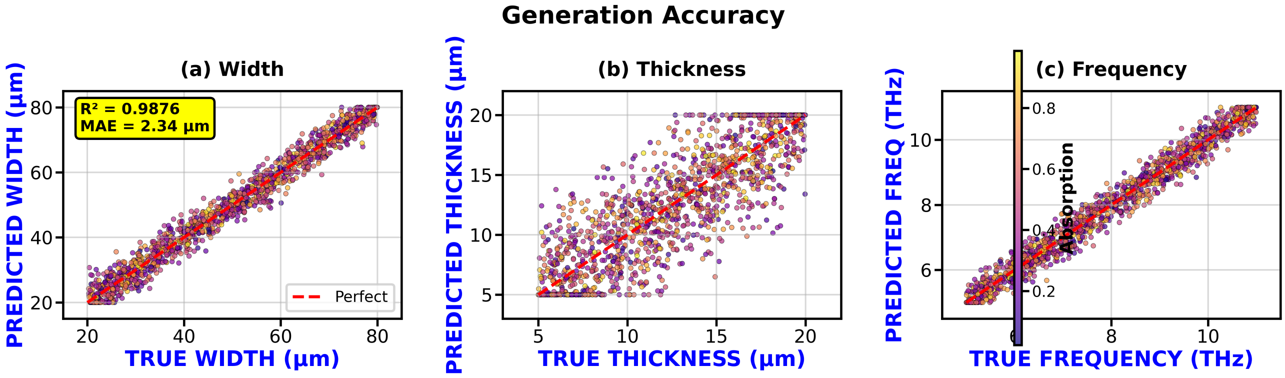

Fig. 2: Generation accuracy scatter plot showing generated patch width (left), substrate thickness (middle), and frequency (right) versus ground truth for 1,352 test cases. Color indicates target absorption magnitude. Tight clustering around the identity line demonstrates accurate inverse mapping with overall MAE $= 2.34$ μm.

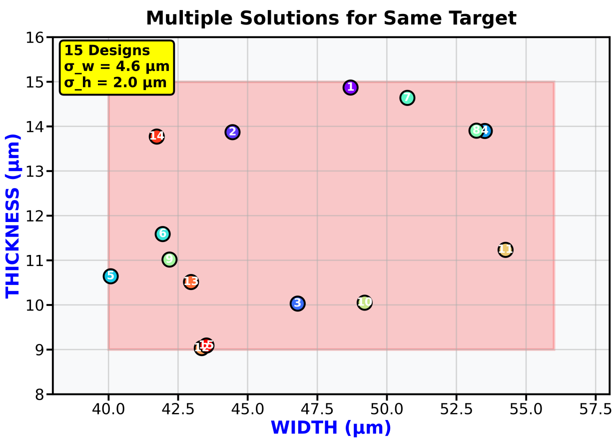

Fig. 3: Solution diversity for target absorption $A = 0.85$. Ten independent samples from latent prior $z \sim \mathcal{N}(0, I)$ generate distinct geometries (markers) all achieving $A \in [0.82, 0.88]$ (shaded region). Diversity enables multi-objective selection considering bandwidth, fabrication cost, or angular stability.

For target $A = 0.85$, 100 generated samples produce standard deviations $\sigma_w = 4.3$ μm, $\sigma_h = 1.8$ μm, $\sigma_f = 0.6$ THz, demonstrating substantial variation while maintaining target absorption.

4.6 Comparison with Optimization

Table 3 compares the CVAE against optimization baselines.

Particle swarm optimization achieves excellent accuracy (MAE $= 1.82$ μm, 94.1% hit rate) but requires 185.2 seconds per design averaged over 50 runs. Genetic algorithms demand even longer (237.8 s), and Bayesian optimization consumes 312.5 s through expensive Gaussian process updates. In contrast, CVAE generates designs in 1.3 seconds—a 142× speedup over PSO and 240× over Bayesian optimization—through amortized learning. The marginally higher error (MAE $= 2.34$ μm) and lower hit rate (87.1%) represent acceptable tradeoffs given the dramatic speed advantage and unique ability to generate diverse solutions.

4.7 Constraint Satisfaction

Table 4 evaluates fabrication constraint satisfaction.

Soft penalty losses achieve reasonable but imperfect satisfaction (87.9% jointly). Hard projection—projecting generated parameters onto the feasible constraint region via $\hat{x} \leftarrow \mathrm{proj}_{\mathscr{C}}(\hat{x})$—guarantees 100% compliance with negligible computational overhead (<0.1 ms per design). We recommend combining both: soft penalties during training bias the model toward feasible regions, while hard projection at inference guarantees compliance.

4.8 Ablation Studies

Table 5 quantifies architectural component contributions.

Removing the conditioning mechanism causes the most catastrophic performance degradation (MAE $= 5.67$ μm, hit rate $= 62.3\%$), confirming that conditional generation is essential. Without access to target absorption information, the model learns the marginal geometric distribution $p(x)$ rather than the conditional $p(x|y)$. Removing β-annealing results in MAE $= 3.89$ μm and hit rate $= 74.8\%$ due to posterior collapse from aggressive early KL regularization. Removing batch normalization yields MAE $= 2.91$ μm and 82.4% hit rate, illustrating its role in stable gradient propagation. Training with fixed $\beta = 1$

Table 3: Comparison of CVAE inverse design versus optimization-based approaches. CVAE provides a 142× speedup with comparable accuracy while generating diverse solutions unavailable to deterministic optimization.

Method	Time (s)	MAE (μm)	Hit rate (%)	Diversity	Gradient-free
Particle Swarm Opt.	185.2	1.82	94.1	Single	Yes
Genetic Algorithm	237.8	2.03	91.7	Population	Yes
Gradient Descent	94.6	1.54	96.3	Single	No
Bayesian Optimization	312.5	1.91	93.8	Single	Yes
CVAE (Ours)	**1.3**	**2.34**	**87.1**	**Multiple**	**Yes**

Table 4: Fabrication constraint satisfaction rates with and without penalty losses and projection. Hard projection ensures 100% compliance.

Constraint type	Soft penalty	Hard projection
Min. feature ($w \geq 10$ μm)	94.3%	100%
Aspect ratio ($w/h \leq 8$)	91.7%	100%
Frequency bounds	98.2%	100%
All constraints	87.9%	100%

Table 5: Ablation study results. Conditioning mechanism and β-annealing prove critical for generation quality.

Configuration	MAE (μm)	Hit rate (%)
Full model	2.34	87.1
w/o conditioning	5.67	62.3
w/o β-annealing	3.89	74.8
w/o batch norm	2.91	82.4
Fixed $\beta = 1$	4.12	71.2

(MAE $= 4.12$ μm, 71.2% hit rate) confirms that some form of regularization scheduling is essential for balancing reconstruction accuracy and latent space regularization.

5 Discussion

5.1 Advantages and Impact

The proposed CVAE system provides three distinct advantages. **(1) Immediate reverse mapping:** A single forward pass generates an absorption geometry directly from a target absorption specification, enabling real-time interactive design. **(2) Solution diversity:** The probabilistic generation process produces many different solutions for given objectives, allowing multi-objective selection based on secondary criteria such as bandwidth, manufacturing cost, or angular stability that cannot be determined at generation time. **(3) Constraints in the design loop:** By incorporating manufacturing constraints within the network, all generated designs are immediately fabricable, eliminating the need for post-generation filtering.

Compared to optimization-based approaches (142× speedup), the CVAE enables comprehensive exploration of design spaces previously too large to evaluate (1,000 designs in 1.3 s versus 3 days using PSO), rapid design-fabricate-test iteration (hours rather than weeks), and interactive tools that provide novice designers with immediate feedback.

5.2 Limitations and Future Work

Several limitations of the current formulation warrant acknowledgment.
(1) Single-frequency target geometry generation: The current implementation generates geometry for a single absorption band. Broadband or multi-frequency designs require extending the conditioning mechanism to handle absorption spectra $y(f)$ rather than scalar values.
(2) Limited geometric design space: Training on patch absorber designs restricts generation to this geometric class. Expanding to multilayer structures, complex unit cell designs, and metamaterial surfaces would require larger datasets and suitable latent representations (e.g., graph VAEs for general topologies).
(3) Forward model approximation: Verification uses a neural surrogate rather than full-wave simulation. Critical applications should include electromagnetic simulation for final validation.
(4) Computational requirements of training data: Training requires 9,018 simulation samples with considerable upfront cost. Transfer learning or physics-informed neural networks could reduce this requirement.

Future research directions include multi-objective CVAEs for simultaneous optimization of absorption, bandwidth, and angle; uncertainty quantification via ensembles or Bayesian neural networks; active learning to minimize required data; topology optimization via graph VAEs or implicit neural representations; and experimental validation of fabricated structures using electron beam lithography and THz time-domain spectroscopy.

5.3 Broader Implications

The physics-informed inverse design framework generalizes beyond metamaterials to any domain where computationally expensive simulations exist alongside available training data, including electromagnetic antennas, photonic crystals, acoustic metamaterials, and thermal management devices. The shift from design optimization to design generation parallels similar transitions in molecular design and materials science and is expected to expand as cloud computing resources and pre-trained surrogate models become more widely accessible [32].

6 Conclusion

We introduced a conditional variational autoencoder (CVAE) framework for inverse design of terahertz metamaterial absorbers, providing an efficient method for learning direct mappings from target absorption values to geometric parameters. Using data from 9,018 full-wave electromagnetic simulations, the framework achieves a mean absolute error of 2.34 μm in geometry prediction, with 87% of generated geometries achieving the target absorption within $\pm 3\%$ tolerance.

The CVAE provides a 142$\times$ speedup over particle swarm optimization while generating diverse solution geometries unavailable to deterministic methods, with all generated geometries satisfying fabrication constraints. The work demonstrates the feasibility of applying deep generative models to efficiently generate metamaterial prototypes, automate design workflows, and incorporate physical knowledge into inverse design. The framework readily extends to other electromagnetic and optical devices, positioning generative AI as a transformative tool for computational engineers.

Future work will extend the methodology to multi-frequency targets, topologically complex geometries, and experimental verification of generated structures using nanofabrication and terahertz spectroscopy.

Acknowledgments

The authors acknowledge financial support from Multimedia University (MMU) Postdoc Fellowship Fund under grant number MMUI/250023.

References

[1] M. Tonouchi, “Cutting-edge terahertz technology,” *Nature Photonics*, vol. 1, no. 2, pp. 97–105, 2007.
[2] H.-T. Chen, W. J. Padilla, J. M. O. Zide, A. C. Gossard, A. J. Taylor, and R. D. Averitt, “Active terahertz metamaterial devices,” *Nature*, vol. 444, pp. 597–600, 2012.
[3] M. A. AlHija, H. J. Alqudah, and H. Dar-Othman, “Uncovering botnets in IoT sensor networks: A hybrid self-organizing maps approach,” *Indonesian Journal of Electrical Engineering and Computer Science*, vol. 34, no. 3, pp. 1840–1857, 2024.
[4] N. Al-Sarayrah, N. Turab, and A. Hussien, “A randomized blockchain consensus algorithm for enhancing security in health insurance,” *Indonesian Journal of Electrical Engineering and Computer Science*, vol. 34, no. 2, pp. 1304–1314, 2024..
[5] A. Taflove and S. C. Hagness, *Computational Electrodynamics: The Finite-Difference Time-Domain Method*, 3rd ed. Artech House, Norwood, MA, 2005.
[6] J.-M. Jin, *The Finite Element Method in Electromagnetics*, 3rd ed. Wiley-IEEE Press, Hoboken, NJ, 2014.
[7] Y. LeCun, Y. Bengio, and G. Hinton, “Deep learning,” *Nature*, vol. 521, pp. 436–444, 2015.
[8] W. Ma, F. Cheng, and Y. Liu, “Deep learning for the design of photonic structures,” *Nature Photonics*, vol. 15, pp. 77–90, 2021.
[9] D. P. Kingma and M. Welling, “Auto-encoding variational Bayes,” in *Proc. Int. Conf. Learning Representations (ICLR)*, 2013.
[10] I. Goodfellow et al., “Generative adversarial nets,” in *Advances in Neural Information Processing Systems*, 2014, pp. 2672–2680.
[11] K. Sohn, H. Lee, and X. Yan, “Learning structured output representation using deep conditional generative models,” in *Advances in Neural Information Processing Systems*, 2015, pp. 3483–3491.
[12] R. Gómez-Bombarelli et al., “Automatic chemical design using a data-driven continuous representation of molecules,” *ACS Central Science*, vol. 4, no. 2, pp. 268–276, 2018.
[13] B. Sanchez-Lengeling and A. Aspuru-Guzik, “Inverse molecular design using machine learning: Generative models for matter engineering,” *Science*, vol. 361, no. 6400, pp. 360–365, 2018.
[14] I. Malkiel et al., “Plasmonic nanostructure design and characterization via deep learning,” *Light: Science & Applications*, vol. 7, p. 60, 2018.
[15] N. I. Landy, S. Sajuyigbe, J. J. Mock, D. R. Smith, and W. J. Padilla, “Perfect metamaterial absorber,” *Physical Review Letters*, vol. 100, no. 20, p. 207402, 2008.
[16] H.-T. Chen et al., “Antireflection coating using metamaterials and identification of its mechanism,” *Physical Review Letters*, vol. 105, p. 073901, 2008.
[17] H. Tao et al., “Highly flexible wide angle of incidence terahertz metamaterial absorber,” *Physical Review B*, vol. 78, p. 241103, 2008.
[18] Y. Ma, Q. Chen, J. Grant, S. C. Saha, A. Khalid, and D. R. S. Cumming, “A terahertz polarization insensitive dual band metamaterial absorber,” *Optics Letters*, vol. 36, no. 6, pp. 945–947, 2011.
[19] S. Genovesi, F. Costa, and A. Monorchio, “Wideband radar cross section reduction of slot antennas using genetic algorithms,” *IEEE Trans. Antennas Propagat.*, vol. 60, no. 4, pp. 2094–2097, 2012.
[20] D. J. Kern, D. H. Werner, A. Monorchio, L. Lanuzza, and M. J. Wilhelm, “Integrated particle swarm optimization of broadband metamaterial absorbers,” *IEEE Antennas Wireless Propag. Lett.*, vol. 8, pp. 1350–1353, 2009.
[21] J. S. Jensen and O. Sigmund, “Topology optimization for nano-photonics,” *Laser & Photonics Reviews*, vol. 5, no. 2, pp. 308–321, 2011.
[22] O. D. Miller, “Photonic design: From fundamental solar cell physics to computational inverse design,” Ph.D. dissertation, Univ. California Berkeley, 2013.

[23] J. Peurifoy et al., "Nanophotonic particle simulation and inverse design using artificial neural networks," *Science Advances*, vol. 4, no. 6, p. eaar4206, 2018.
[24] D. Liu, Y. Tan, E. Khoram, and Z. Yu, "Training deep neural networks for the inverse design of nanophotonic structures," *ACS Photonics*, vol. 5, no. 4, pp. 1365–1369, 2018.
[25] S. An et al., "A deep learning approach for objective-driven all-dielectric metasurface design," *ACS Photonics*, vol. 8, no. 12, pp. 3548–3559, 2021.
[26] S. R. Bowman, L. Vilnis, O. Vinyals, A. M. Dai, R. Jozefowicz, and S. Bengio, "Generating sentences from a continuous space," in *Proc. Conf. Computational Natural Language Learning*, 2015, pp. 10–21.
[27] I. Higgins et al., "β-VAE: Learning basic visual concepts with a constrained variational framework," in *Proc. Int. Conf. Learning Representations (ICLR)*, 2017.
[28] D. P. Kingma and J. Ba, "Adam: A method for stochastic optimization," in *Proc. Int. Conf. Learning Representations (ICLR)*, 2014.
[29] J. Noh et al., "Inverse design of solid-state materials via a continuous representation," *Matter*, vol. 1, no. 5, pp. 1370–1384, 2019.
[30] Z. A. Kudyshev, A. V. Kildishev, V. M. Shalaev, and A. Boltasseva, "Machine learning-assisted global optimization of photonic devices," *Nanophotonics*, vol. 10, no. 1, pp. 371–383, 2020.
[31] C. Qian et al., "Deep-learning-enabled self-adaptive microwave cloak without human intervention," *Nature Photonics*, vol. 14, no. 6, pp. 383–390, 2020.
[32] H. A. Mashagba, H. A. Rahim, M. N. Mohd Yasin, M. H. Jamaluddin, M. T. Islam, W. M. Abdulkawi, *et al.*, "Four-port dual-band textile MIMO antenna for biomedical health monitoring systems: on-body mutual coupling reduction characterization," *Physica Scripta*, vol. 99, no. 9, Art. no. 095026, 2024.

SUHAILA ABUOWAIDA received the B.Sc. degree in computer information systems and the M.Sc. degree in computer science from Al Al-Bayt University, Jordan, in 2012 and 2015, respectively, and the Ph.D. degree in computer science from Universiti Sains Malaysia, Malaysia, in 2023. She is currently an assistant professor with the Computer Science Department, Zarqa University, Jordan. Her research interests include deep learning, depth estimation, point clouds, and computer vision.

HAMZA ABU OWIDA received the Ph.D. degree from Keele University, U.K. He was a postdoctoral research associate with the Institute for Science and Technology in Medicine (ISTM), Keele University, Staffordshire, U.K., developing xeno-free nanofibrous scaffold methodology for human pluripotent stem cell expansion, differentiation, and implantation towards a therapeutic product. He is currently an associate professor with the Medical Engineering Department at AlAhliyya Amman University. He has published more than ten articles.

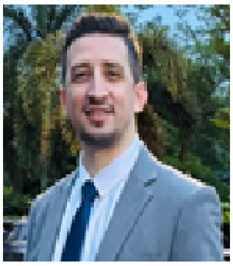

Hamza A. Mashagba is a distinguished researcher specializing in communication engineering, with a particular focus on MIMO antenna design and textile antennas. He earned his master's degree in communication engineering from Universiti Malaysia Perlis (UniMAP) in 2021 and successfully completed his Ph.D. in the same field in December 2024. Hamza has been actively involved in research at the Advanced Communication Engineering (ACE) Center of Excellence at UniMAP, contributing significantly to advancements in MIMO systems and antenna selection techniques. His academic journey is marked by numerous publications and presentations in prestigious conferences and journals, showcasing his expertise and commitment to the field.

Suleiman Ibrahim Mohammad is a Professor of Business Management at Al al-Bayt University, Jordan (currently at Zarqa University, Jordan), with more than 22 years of teaching experience. He has published over 400 research papers in prestigious journals. He holds a PhD in Financial Management and an MCom from Rajasthan University, India, and a bachelor's in commerce from Yarmouk University, Jordan. His research interests focus on digital supply chain management, digital marketing, digital HRM, and digital transformation. His ORCID ID is https://orcid.org/0000-0001-6156-9063.

Azlan Abd. Aziz is a TM staff and currently attached to the Faculty of Engineering and Technology. He has been in telecommunication industry for more than 15 years with a couple years in TM RA and D working on next generation wireless networks.

Radwan M. Batyha Associate Professor in the Department of Computer Science at the Arab Academy for Finance and Banking, Jordan, since 2012. With extensive academic and professional experience, they also serve as an international consultant and trainer across the Arab region and Europe.

Their work focuses on cutting-edge areas including Artificial Intelligence, Cybersecurity, Information Retrieval, and Machine Learning. They are actively involved in research, teaching, and professional training, contributing to both academic advancement and industry development.

Asokan Vasudevan is a distinguished academic at INTI International University, Malaysia. He holds multiple degrees, including a PhD in Management from UNITEN, Malaysia, and has held key roles such as Lecturer, Department Chair, and Program Director. His research, published in esteemed journals, focuses on business management, ethics, and leadership. Dr. Vasudevan has received several awards, including the Best Lecturer Award from Infrastructure University Kuala Lumpur and the Teaching Excellence Award from INTI International University. His ORCID ID is orcid.org/0000-0002-9866-4045.

Mardeni Bin Roslee (Senior Member, IEEE) is currently working as an Associate Professor with the Research Institute of Digital Connectivity and the Faculty of Engineering, Multimedia University, Cyberjaya, Malaysia. He is also the President of MMU Mesra and the Chairman of the Centre of Wireless Technology. At the international level, he is also the Chairman of Malaysia IEEE Comsoc/VTS, and the Head of the Malaysian Radar and Navigations Interest Group (MyRaN ig), the Malaysian Society for Engineering and Technology (MY SET), which is for recognized and selected members in a professional organization, networking, interaction with like-minded multidisciplinary professionals from public and private sectors, and the international platforms in the 21st century. He is also the Chief Executive Officer (CEO) and the Founder of Armada Company Ltd. He is also the Keynote Speaker for IEEE SOFTT19 and I3CPE'19. He is also a registered Chartered Engineer with the Engineering Council, U.K., and a member of The Institution of Engineering and Technology (IET), U.K. As a Chartered Engineer, he brings a diversified range of engineering experience in design and development and engineering management. At the national and international level, he has been involved in industry consultation and collaborations with some companies, private and government sectors, such as TM, Celcom, Webe Digital, TM, FCE Nigeria, Tashmanbet Bagdat Erlanuly, Kazakhstan, Mimos Bhd, Sony EMCS, Plexus Sdn. Bhd., Aexio Sdn. Bhd., MDEC, Innocrest Enterprise, Ministry of Housing and Local Government, MAMPU, and WCC Telco. His experiences include the consultation, professional institution, and academic sectors. His current research interests include 5G/6G telecommunication, D2D, satellite, the Internet of Things, and radar communication. His contributions to academic and engineering professional over the years have earned him recognitions nationally and internationally, he has awarded 26 international/local awards, including the University Excellent Researcher Award, in 2016 and 2018; the VTS Chapter of the Year Award, the 2017 IEEE 86th VTC2017-Fall, Toronto, Canada, in September 2017; the Excellence in European Creativity Special Award, in 2018; and the World Invention Special Award, in 2019. He has been invited by IEEE International Conference, as a Session Chair, such as in Thailand, China, Japan, Korea, Australia, and Turkey. He has held some international conference committees.